Supplementary Information for

DROOPY LEAF1 Controls Leaf Architecture by Orchestrating Early Brassinosteroid Signaling

Authors: Meicheng Zhao[a,b,1], Sha Tang[b,1], Haoshan Zhang[b,1], Miaomiao He[b,c], Jihong Liu[b,d], Hui Zhi[b], Yi Sui[b], Xiaotong Liu[b], Guanqing Jia[b], Zhiying Zhao[d], Jijun Yan[e,f], Baocai Zhang[e,f], Yihua Zhou[e,f], Jinfang Chu[e,f], Xingchun Wang[c], Baohua Zhao[d], Wenqiang Tang[d], Jiayang Li[e,f], Chuanyin Wu[b,2], Xigang Liu[d,g,2], and Xianmin Diao[b,2]

Corresponding authors: Chuanyin Wu (C.W.); Xigang Liu; Xianmin Diao (X.D.)

Email: wuchuanyin@caas.cn; xgliu@sjziam.ac.cn; diaoxianmin@caas.cn;

This PDF file includes:

Other supplementary materials include Dataset S1

Dataset S1. Primers used in this study

www.pnas.org/cgi/doi/10.1073/pnas.2002278117

SI Materials and Methods

Plant materials and growth conditions

Foxtail millet (*Setaria italica*) variety 'Yugu1' (WT) was used in this study. Yugu1 is a popular commercial cultivar with a decoded genome sequence that is publicly available as a *Setaria* reference (1). The *dpy1* (*droopy leaf 1*) mutant was isolated by screening an EMS-mutated Yugu1 population, followed by 3 backcrosses with Yugu1. All of the plants were grown at the experimental station of the Institute of Crop Sciences in Beijing (116 21′E, 39 54′N) during summer seasons or under long-day greenhouse conditions (16 h light at 28°C and 8 h dark at 24°C) at a light intensity of 100–150 mmol/m^2 s. For BL treatment, seedlings were germinated on moistened filter paper with a 16/8-h light/dark cycle at 28/24°C for 5 days, transferred to a tissue plate with 2 mL of water overnight, and then treated with 5 μM BL or H_2O for the indicated time for time-course experiments.

Map-based cloning of *DPY1*

We crossed *dpy1* with the cultivar SSR41 to produce an F_2 population. Using 116 recessive F_2 plants with the typical droopy leaf phenotype, *DPY1* was initially mapped to a 7.0 Mb interval between the molecular markers IndelM1 and IndelM2 on chromosome 5. Seven new markers were further developed within this interval and *dpy1* was finally narrowed down to a 200 kb region between IndelM7 and MPGD4. BSA-seq was then performed to identify the causal mutation in *dpy1*. Briefly, *dpy1* was backcrossed with its wild-type Yugu1 to generate a BC_1F_2 population. Thirty recessive individuals were selected to generate a DNA pool. High-throughput sequencing was performed on Illumina HiSeq 2500 using the 150-bp paired-end method. The minimum sequencing depth was 30× coverage of the *Setaria* genome. Sequencing read alignment, SNP calling, SNP-index calculation, and data statistics were performed according to the MutMap protocol (2). Primers used for map-based cloning are listed in Dataset S1.

Bioinformatics analysis of DPY1

The DPY1 protein sequence was analyzed with the SMART program (http://smart.embl-heidelberg.de/) for domain prediction. For phylogenetic analysis, the full-length protein sequences were aligned using MUSCLE (3). A maximum likelihood phylogenetic tree was constructed using Mega X (1000 bootstrap replications, and JTT model).

Constructs preparation and plants transformation

To generate a *DPY1* knockout construct, oligonucleotides used for targeted mutagenesis were designed using the online software (http://cbi.hzau.edu.cn/crispr/) and cloned into a *CRISPR-Cas9* vector. To generate *Ubi::DPY1-3FLAG* and *35S::SiBZR1-GFP*, the corresponding ORFs were amplified from cDNA of a Yugu1 plant. The *DPY1* fragment was subcloned into a modified binary vector *pTCK303* with 3 repeats of FLAG tags downstream of the insertion. The *SiBZR1* fragment was first subcloned into an intermediate vector *pENTR1A* (Invitrogen) and transferred into the destination vector *pEarleyGate 103* by a recombination reaction (Invitrogen, 11791020). For the complementation vector, a 7.0 kb genomic fragment, including a 2.2 kb promoter region, was amplified from Yugu1 and cloned into a modified binary vector *pCAMBIA1305.1-EGFP*, in-frame fused with downstream GFP, resulting in *DPY1::DPY1-GFP*. To generate a *DPY1::GUS* construct, a 2.8 kb promoter region of *DPY1* from Yugu1 was cloned into the binary vector *pCAMBIA1305* upstream of the *GUS* reporter gene. All resulting constructs were verified by sequencing and transformed into *Agrobacterium tumefaciens* strain EHA105 for foxtail millet transformation. Expression of transgenes in foxtail millet plants was further verified by immunoblot detection. Primers used for plasmid construction are listed in Dataset S1.

BR/BRZ treatment

For skotomorphogenesis, seeds of WT and *dpy1* were sowed on filter paper in petri dishes soaked with a series of concentrations of BL/BRZ. Coleoptile length was measured 5 days after germination in the dark at 28°C. For leaf curvature determination, WT and *dpy1* seedlings were sprayed with 5 μM BL or BRZ for three days with three times at a 24-hour interval, and then the second leaf from top was measured for the proximal-distal distance (PDD) and full length (FL). The ratio of PDD to FL was used to quantify bending degree of the leaf.

Anatomical observation of leaf

Blades of the second leaf from the top were fixed in FAA solution, dehydrated in graded ethanol, and embedded in paraffin. Microtome sections (10 μm) were applied to poly-lysine-coated slides. After dehydration by a graded ethanol series, the sections were strain with toluidine blue. Cross-sections were strained by hand with 1% phloroglucinol (w/v) in 12% HCl and observed with a microscope under white light. Phloroglucinol-HCl staining was performed as previously described (4).

Cell wall composition analysis

The leaf blades collected from Yugu1 and *dpy1* plants at the 5 leaf stage were dried in a 65°C oven for 2 days and ground to fine powders. Cell wall compositions, including cellulose, saccharide, and lignin, were measured as described previously (5).

RNA-Seq and qRT-PCR analysis

Two-week-old WT and *dpy1* plants were sprayed with 1 μM BL or water three times in a 12-hour interval. Ten independent leaves were collected for each of the three replicates and immediately frozen in liquid nitrogen for RNA extraction. Total RNA was isolated by the standard TRIzol method (Invitrogen) and integrity was evaluated using a Bioanalyzer 2100 (Agilent Technologies). Construction of cDNA libraries and high-throughput sequencing (150 bp paired-end reads) using HiSeq 2500 were outsourced to Berry Genomics (Beijing). For each sample, an average of 5.0 gigabases of raw data were generated. Clean sequencing reads were aligned to the *Setaria* reference genome V2.2 (https://phytozome.jgi.doe.gov) and then were analyzed according to previously reported (6). A total of 26,954 genes were identified, representing 79.5% of all predicted genes in foxtail millet. SiBZR1 target genes were determined by the homolog blast of BZR1 target genes in Arabidopsis (7). Mev tools (http://mev.tm4.org) were employed for Heatmap construction of DEGs. For qRT-PCR, total RNA was extracted from the indicated tissues or plants and treated with DNaseI to remove contaminating DNA. RevertAid RT Reverse Transcription Kit (Thermo Scientific) was used for reverse transcription. Quantitative real-time PCR was performed on the Biorad CFX-96 Real-Time PCR system (Bio-Rad) using the SYBR Green supermix (DBI Bioscience). Gene expression level was normalized with the foxtail millet *actin* gene (Seita.7G294000). Primers used for RT-PCR are listed in Dataset S1.

Protoplast transient expression, *in vivo* phosphorylation detection, Co-Immunoprecipitation (IP), and LC-MS/MS assay

For their transient expression in protoplasts, full-length cDNA of *DPY1* and *SiBAK1* was generated from WT plants and fused in-frame with the GFP or HA tag in transient expression vectors to generate *35S::DPY1-GFP*, or *35S::SiBAK1-HA*, respectively. The construct (10 μg each) was introduced into protoplasts prepared from two-week-old foxtail millet leaves as previously reported (8). For DPY1 subcellular localization examination, the infected protoplasts were observed under a confocal fluorescence microscope (Leica TCS SP7) to monitor GFP signals. For endogenous SiBRI1 phosphorylation detection, two-week-old seedlings were ground and incubated with phosphorylation buffer (50 mM Tris-HCl, pH 7.6, 150 mM NaCl, 10% glycerol, 0.1% NP-40, 1% Triton X-100, 1× Complete Protease Inhibitor Cocktail, and 1× Phosphatase Inhibitor Cocktail) for 1h at 4°C with constant rotation. Total cell lysates were obtained by centrifugation at 12,000 rpm for 15 min at 4°C, and then incubated with anti-SiBRI1 antibody

overnight. The phosphorylation of immunoprecipitated SiBRI1 was detected by immunoblotting using an anti-Phospho-Threonine (pThr) antibody (Cell Signaling technology, Cat. No. ab9381, dilution: 1:2000). For the DPY1-SiBAK1 Co-IP experiment, DPY1-GFP and SiBAK1-HA were co-expressed in foxtail millet leaf protoplasts overnight and then treated with or without 5 μM BL for 2 h. For the SiBAK1-SiBRI1 Co-IP experiment, SiBAK1-HA was expressed in leaf protoplasts of WT or *dpy1* overnight and treated with or without BL for 2 h. Protoplasts containing target proteins were collected and incubated with phosphorylation buffer without a Phosphatase inhibitor. Co-immunoprecipitated products with the GFP-Trap or anti-HA antibody were detected by immunoblotting using anti-HA (abcam, Cat. No. ab173826, dilution: 1:2000), anti-GFP (abcam, Cat. No. ab6663, dilution: 1:2000) or anti-SiBRI1 antibody (dilution: 1:3000), respectively. For LC-MS analysis, the same amount of WT and *Ubi::DPY-3FLAG* plants (5 μg fresh blade for each sample) were ground to fine powder to extract total soluble proteins as described above. The supernatant was incubated with Anti-FLAG M2 Affinity Gel (Sigma-Aldrich, Cat. No. A2220). Immunoprecipitated products were extensively washed and then eluted with 3×FLAG peptide (Sigma-Aldrich, Cat. No. 4799). The eluted proteins were digested by trypsin and separated using a Thermo Scientific EASY-nLc 1000 System. The raw data were processed using MaxQuant software with the settings as described (9). Outputs were searched against the foxtail millet proteome database. (https://www.ncbi.nlm.nih.gov/genome/10982).

Yeast two-hybrid assay

Yeast two-hybrid assays were performed based on a DUAL membrane system (Dualsystems Biotech). The *DPY1* coding region without a signal peptide (aa: 30-633) was amplified and subcloned into *pBT3-SUC* vector between double *SfiI* sites to generate DPY1-Cub. mDPY1-Cub was created by introducing two mutations at 474/475 sites (G474V/T475A) as previously reported in other species into DPY1-Cub (10). Full length coding regions of *SiBAK1* and *SiBRI1* were amplified and subcloned into a *pPR3-C* vector at the *EcoRI* site to generate SiBAK1-NubG and SiBRI1-NubG, respectively. Assays were performed according to instructions by the manufacturer. *pOst1-NubI* (wild-type Nub) was used as control prey to test the correct expression of DPY1-Cub on the membrane. Primers used for plasmid construction are listed in Dataset S1.

BiFC assay

The full-length cDNA of *DPY1*, *SiBAK1,* and *SiCIK4* (Seita.1G023400) were first subcloned into the intermediate vector *pENTR1A* and transferred into the destination vectors *35S::nYFP* and *35S::cYFP* by recombination reaction (Invitrogen, 11791020), respectively, generating constructs nYFP-DPY1, nYFP-SiCIK4, or SiBAK1-cYFP. The resultant constructs and control blank vector were co-expressed in *Nicotiana benthamiana* leaves for 3 days and the fluorescence signal was

observed by a confocal microscope (Leica TCS SP7). Primers used for plasmid construction are listed in Dataset S1.

Recombinant protein preparation, pull-down, and *in vitro* kinase activity assay

The kinase domain (KD) of DPY1 (aa: 280-633), SiBAK1 (aa: 285-631), and SiBRI1 (aa: 719-1117) were amplified from the cDNA of WT plant and shifted into vectors *pET-28a*, *pMAL-C2X,* and *pGEX-4T-1*, respectively, to generate *His-DPY1-KD*, *MBP-SiBAK1-KD,* and *GST-SiBRI1-KD*. The resultant constructs were expressed in the *E. coli* BL21 (DE3) strain and proteins were purified using appropriate agarose beads or resin. The eluted protein was used for *in vitro* pull-down assays. For the DPY1–SiBAK1 interaction test, 2 μg His-DPY1-KD and 5 μg MBP-SiBAK1-KD or MBP tag protein were incubated at 28°C for 30 minutes. For the competitive binding assays with DPY1, 10 μg MBP-SiBAK1-KD and 3 μg GST-SiBRI1-KD coupled with different amounts of His-DPY1-KD (0, 1.5, 10 μg) were mixed together at 28°C for 30 minutes. Pull-down assays were performed using MBP agarose beads (NEB, E8036S). After extensive washing, the precipitated products were analyzed by western blotting using an anti-GST or anti-His antibody (Sigma-Aldrich, Cat. No. G7781/H1029, dilution: 1:5000).

For kinase activity assays, the DPY1 kinase domain (aa: 280-633) and its kinase-dead version (aa: 280-633, G474V/T475A) were cloned into the vector *pGEX-4T-1*, generating *GST-DPY1-KD* and *GST-mDPY1-KD*, respectively. The wild type kinase domain (aa: 285-631) and kinase-dead version (K364E) of SiBAK1 were subcloned into vector *pMAL-C2X* to generate *MBP-SiBAK1-KD* and *MBP-mSiBAK1-KD*, respectively. The recombinant protein was purified by GST or MBP agarose beads and eluted with 10 mM glutathione or maltose. The purified proteins were each incubated for an autophosphorylation test or together for a trans-phosphorylation test. A phosphorylation reaction was set up in 20 μl volume containing 0.5–1.5 μg of each protein, 50mM HEPES (pH 7.5), 10 mM $MgCl_2$, 100 μM $MnCl_2$, 1 mM DTT, and 100 μM ATP. The mixtures were incubated at 28°C for 1–3 h and stopped by adding 2× SDS buffer. Protein phosphorylation analysis was performed by SDS-PAGE separation and immunoblot analysis with anti-pThr or Phos-tag gel (Wako, 304-93521) detection according to the manufacturer's instructions. Primers used for plasmid construction are listed in Dataset S1.

Antibody preparation

To create the anti-SiBRI1 antibody, the unique extracellular domain of SiBRI1 (aa: 110-347) was shifted into vector *pET-28a* to generate *His-SiBRI1* and purified His-SiBRI1 was used to generate the anti-SiBRI1 antibody in a rabbit.

Determination of endogenous BR levels

The quantification of endogenous BR levels was performed based on the method reported previously (11) but simplified in sample pretreatment. The harvested plant materials were first ground to fine powder. Two hundred milligrams of the powder were extracted with 90% aqueous methanol (MeOH) in an ultrasonic bath for 1 hour. Simultaneously, D_3-BL, D_3-CS, D_3-6-deoxo-CS, and D_3-TY were added to the extract as internal standards for BR content measurement. After the MCX cartridge was activated and equilibrated with MeOH, water, and 40% MeOH in sequence, the crude extracts reconstructed in 40% MeOH were loaded onto the cartridge. The MCX cartridge was washed with 40% MeOH and BRs were eluted with MeOH. After being dried with N_2 stream, the eluent was dissolved with ACN to be derivatized with DMAPBA prior to UPLC-MS/MS analysis. BR analysis was performed on a quadrupole linear ion trap hybrid MS (QTRAP 5500, AB SCIEX) equipped with an electrospray ionization source coupled with UPLC (Waters). The UPLC inlet method, ESI source parameters, MRM transitions, and related compound-dependent parameters were set as described in the previous report (11). As for 6-deoxo-CS, D_3-6-deoxo-CS, TY and D_3-TY, the MRM transition 580.4>176.1, 583.4>176.1, 578.5>176.1, and 581.5>176.1 was used for quantification

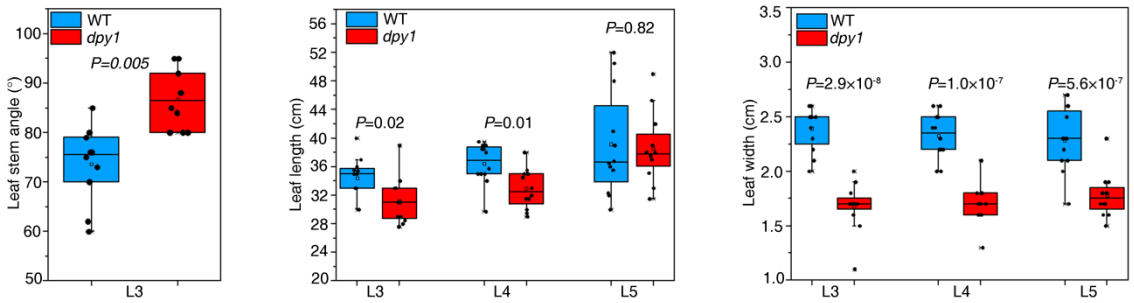

Fig. S1. Comparison of leaf-stem angle, leaf length, and width between WT and *dpy1* adult plants grown in the field. The leaf-stem angles of leaf 3 (L3, counted from the top) were investigated, and the fully expanded leaves (L3–L5) were measured for leaf length and width. The values indicate means ± SD (n = 10 for leaf-stem angle; n = 12 for leaf length and width), with *P*-values based on Student's *t*-tests.

Fig. S2. *dpy1* plants are susceptible to pathogen attack. (**A**) Field-grown *dpy1* plants were more susceptible to the brown streak disease, caused by the bacterial pathogen *Pseudomonas setariae*. Red arrows indicate lesions on leaves. (**B**) A close look of infected *dpy1* leaves.

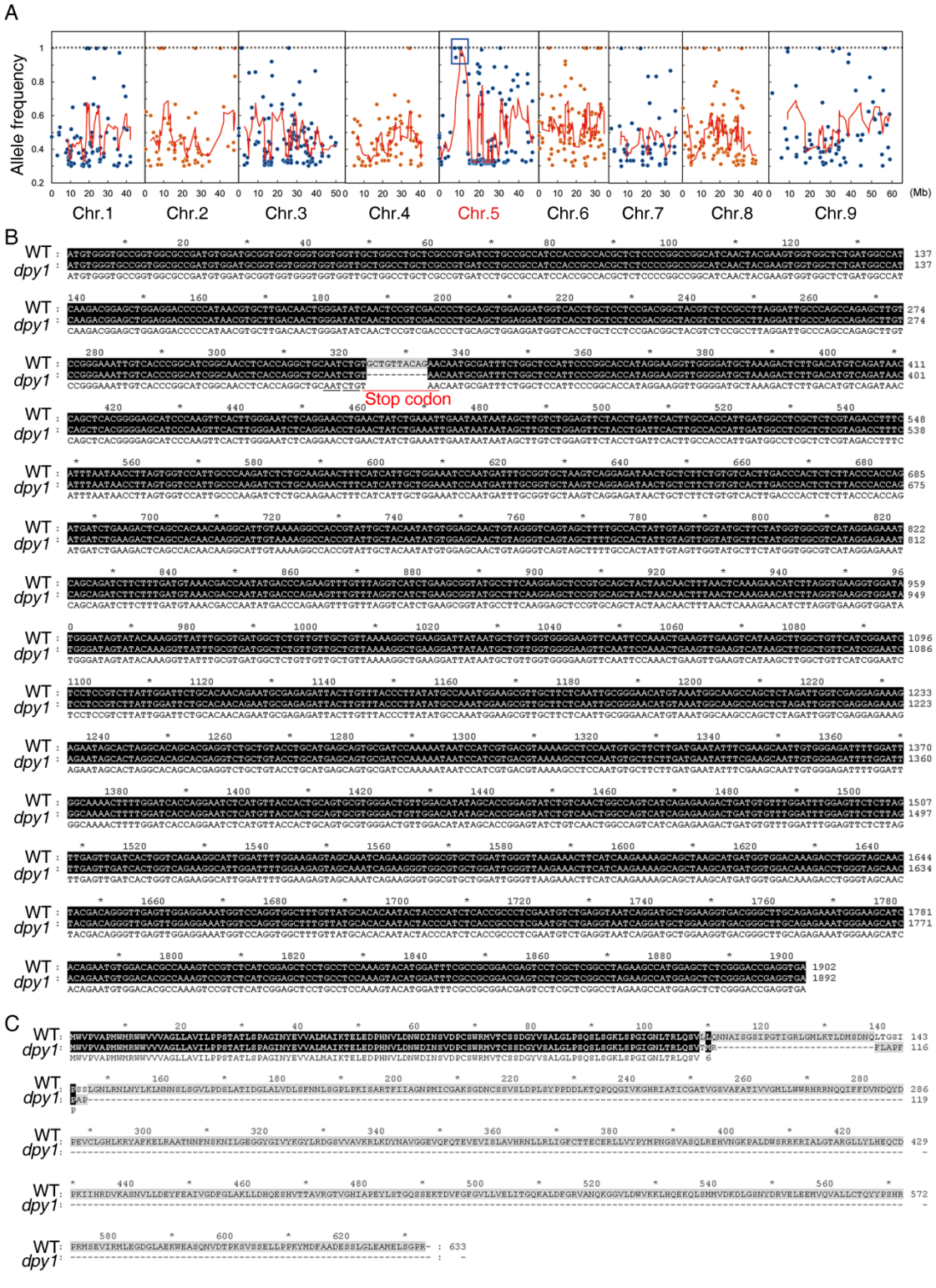

Fig. S3. Cloning and sequence analysis of *dpy1*. (**A**) Cloning of *dpy1* by BSA (Bulk Segregant Analysis). The calculated frequency of mutant alleles and their location on the corresponding

chromosomes are indicated on the y and x axis, respectively. Blue and orange dots represent all of the SNPs found in the *dpy1* mutant genomic pool from a BC_1F_2 population by comparison to the Yugu1 reference genome. The red line represents a smoothed curve over a 5-SNP window. The blue box indicates a peak detected on chromosome 5, which encompasses the mapped 200-kb interval. (**B**) Alignment of the WT *DPY1* open reading frame (ORF) with the cloned *dpy1* cDNA identified a 10-bp deletion in *dpy1* transcripts. The red line indicates an immature stop codon (TAA). (**C**) Alignment of the predicted DPY1 protein sequence between WT and *dpy1*.

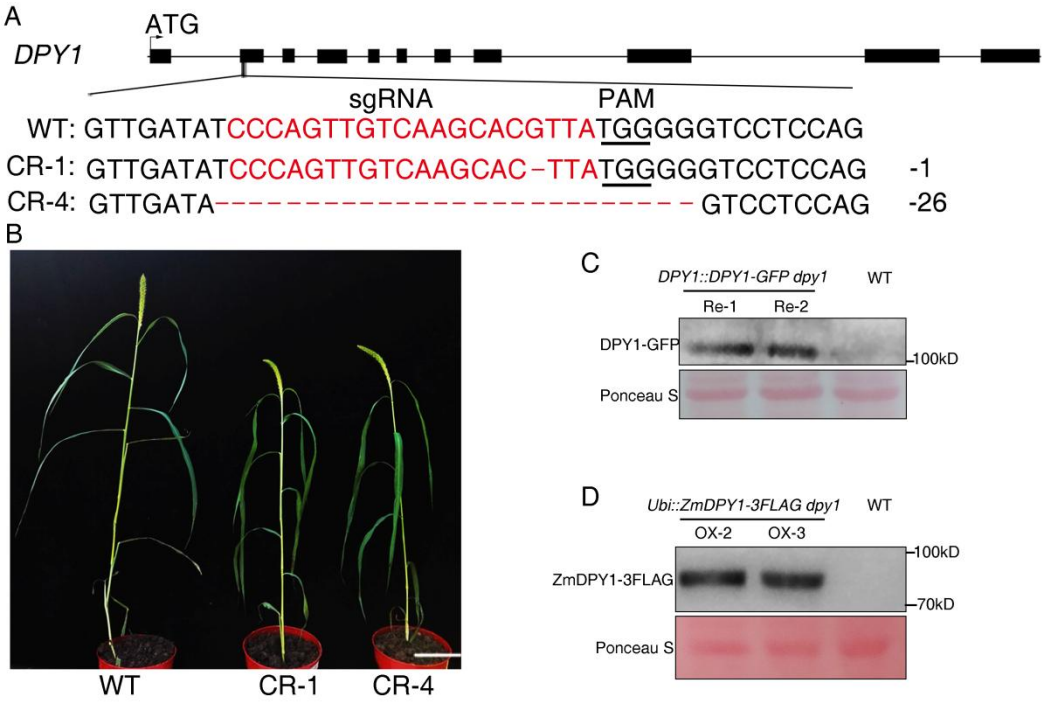

Fig. S4. Verification of CRISPR/*Cas9*-edited *DPY1* plants and *DPY1::DPY1-GFP dpy1* or *Ubi::ZmDPY1-3FLAG dpy1* transgenic plants. (A) CRISPR/*Cas9*-mediated knock-out of *DPY1*. The sgRNA target sequence within the second exon is highlighted in red, and the PAM motif is underlined. The red dashes indicate deleted nucleotides in the two isolated knock-out lines CR-1 and CR-4, and the number of deleted nucleotides is shown to the right. (**B**) DPY1 knock-out plants displayed a similar drooping leaf phenotype as that of *dpy1* at the adult stage. Bar = 10 cm. (**C**) Immunoblot detection of DPY1-GFP in transgenic plants containing *DPY1::DPY1-GFP* using an anti-GFP antibody, with the WT as a control. (**D**) Immunoblot detection of ZmDPY1-3FLAG in transgenic plants containing *Ubi::ZmDPY1-3FLAG* using anti-FLAG antibody, with the WT as a control.

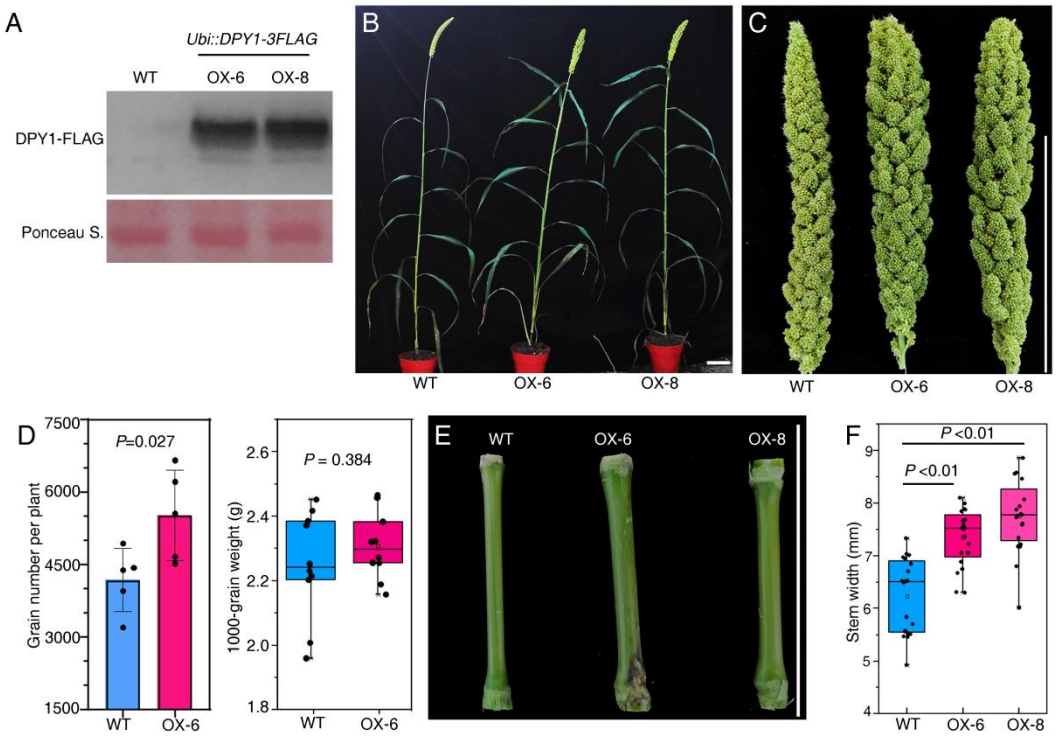

Fig. S5. *DPY1* over-expressing plants have more upright leaves, thicker stems, and bigger panicles. (A) Immunoblotting detection of DPY1-3FLAG in two representative *DPY1* overexpressing transgenic plants (OX-6 and -8) using the anti-FLAG antibody. (**B**) The morphology of OX-6, -8, and WT grown in the field at the adult stage. Bar = 10 cm. (**C**) The bigger panicles of OX-6, -8 compared with the WT. Bar = 10 cm. (**D**) Statistical analysis of the grain number per panicle and 1000-grain weight in OX-6 plants (n = 10). *P*-values were calculated using a Student's *t*-test. (**E**) The thicker stem (the fourth stem counted from the end) of OX-6 and -8 compared with the WT. Bar = 10 cm. (**F**) Statistical analysis of stem width indicated in (E). The values indicate means ± SD (n = 20), with *P*-values based on Student's *t*-tests.

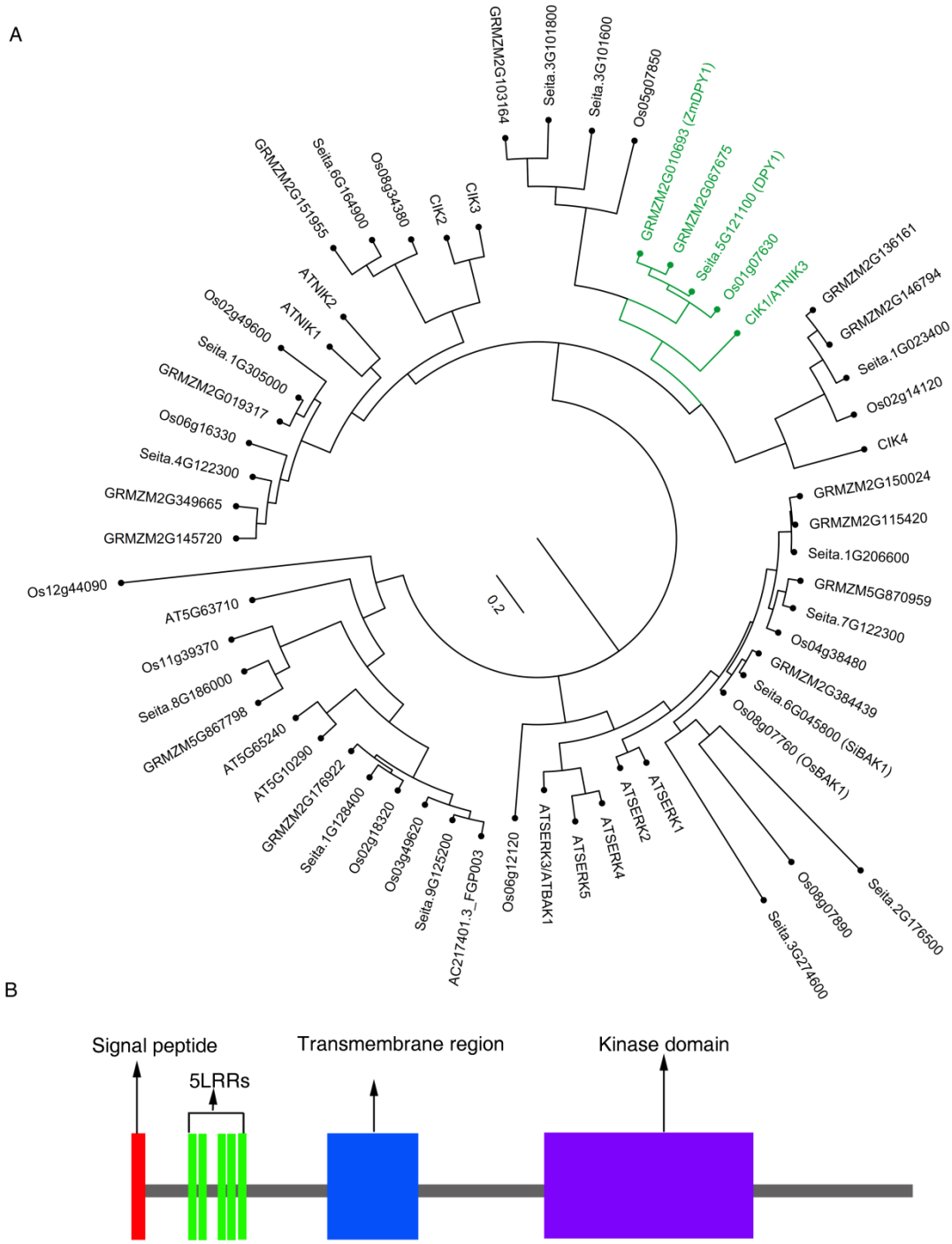

Fig. S6. Bioinformatics analysis of DPY1. (**A**) A phylogenetic tree was constructed based on members of the subfamily II of LRR-RLKs in *Arabidopsis* and their homologs in rice, maize, and foxtail millet. The full-length protein sequences were aligned using MUSCLE. The phylogenetic tree was constructed using Mega X with the maximum likelihood method. **(B)** *DPY1* encodes a

putative plasma membrane protein with a signal peptide, five LRRs, a transmembrane domain, and a kinase domain.

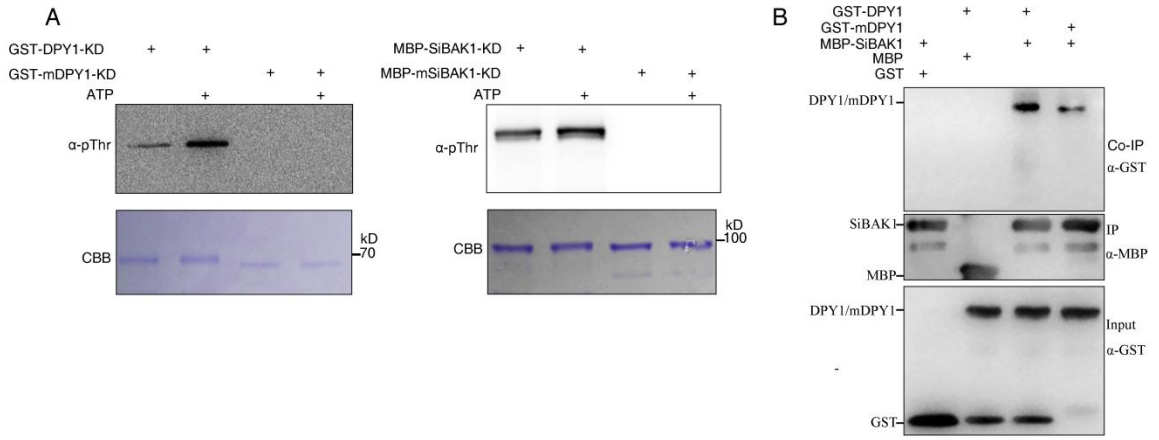

Fig. S7. Kinase activity and interaction of mDPY1 and SiBAK1 in a pull-down assay. (A) Kinase activity examination of DPY1 (left) and SiBAK1 (right). GST-DPY1-KD or its kinase-dead form GST-mDPY1-KD and MBP-SiBAK1-KD or MBP-mSiBAK1-KD were incubated with or without ATP. Phosphorylation detection was performed by immunoblotting using anti-pThr antibody. Purification of the phosphorylated forms of DPY1 and SiBAK1 is indicative of kinase activity and/or autophosphorylation in *E. coli*. Coomassie brilliant blue (CBB) staining indicates the purified recombinant proteins. (**B**) An *in vitro* pull-down assay to examine the interaction of SiBAK1 with DPY1 and mDPY1, respectively. SiBAK1 was immuno-precipitated using anti-MBP first, following by immunoblotting using anti-GST to examine DPY1 and mDPY1, respectively. GST and MBP tag were used as negative controls.

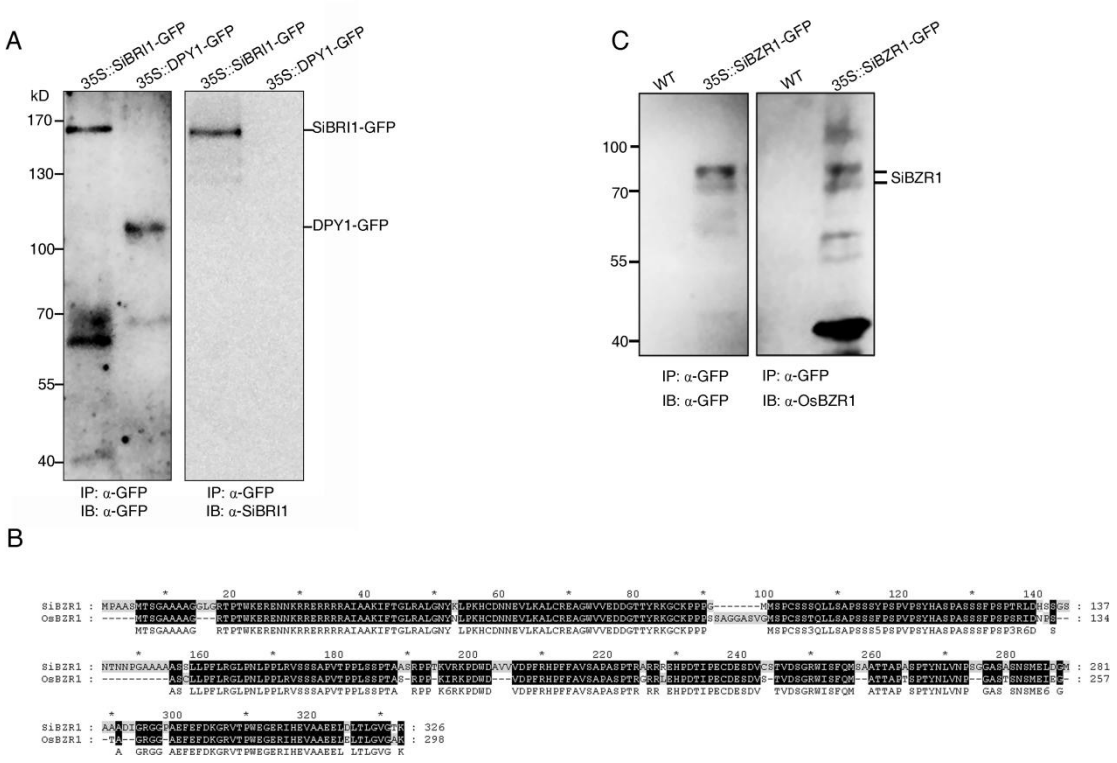

Fig. S8. Validation of anti-SiBRI1 and anti-OsBZR1 antibodies in foxtail millet. (A) The immunoprecipitated (IP) SiBRI1-GFP and DPY1-GFP protein from protoplasts containing *35S::SiBRI1-GFP* and *35S::DPY1-GFP* was detected by immunoblotting (IB) using anti-GFP antibody and anti-SiBRI1 antibody, respectively. (**B**) Alignment of the SiBZR1 and OsBZR1 protein sequences. (**C**) The immunoprecipitated (IP) SiBZR1-GFP protein from *35S::SiBZR1-GFP* transgenic plants were detected by immunoblotting (IB) using an anti-GFP antibody and anti-OsBZR1 antibody, respectively.

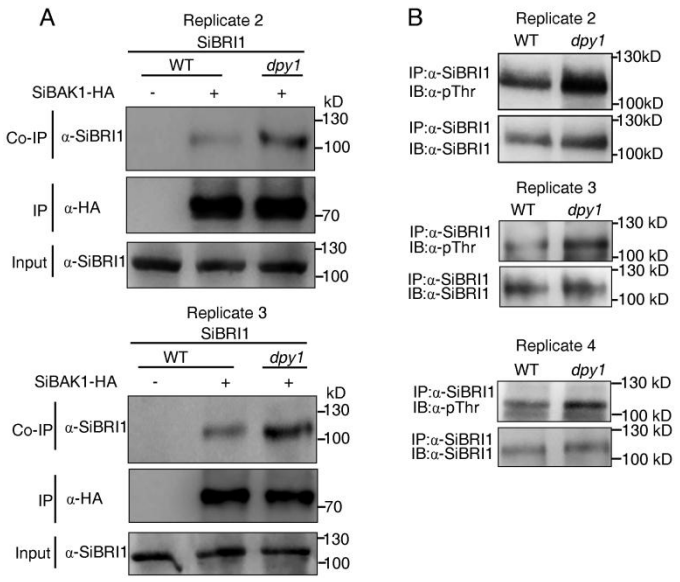

Fig. S9. SiBRI1–SiBAK1 interaction and SiBRI1 phosphorylation are enhanced in *dpy1* plants. (**A**) Co-IP assays in WT and *dpy1* protoplasts revealed the enhanced SiBAK1–SiBRI1 interaction in *dpy1*. Protein extracts from WT or *dpy1* protoplasts transiently expressing *35S::SiBAK1-HA* or the vector control were immunoprecipitated with an anti-HA antibody (IP) and immunoblotted with an anti-SiBRI1 antibody (Co-IP). Biological replicates 2–3 for Fig. 4B. (**B**) Enhanced phosphorylation of endogenous SiBRI1 in *dpy1* plants. SiBRI1 was immunoprecipitated (IP) with an anti-SiBRI1 antibody and its phosphorylation status were determined by immunoblotting (IB) with an anti-pThr antibody. Biological replicates 2–4 for Fig. 4C.

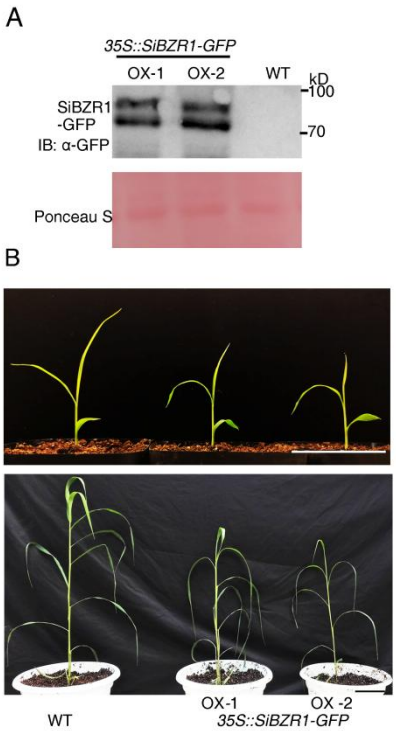

Fig. S10. *SiBZR1* overexpressing plant phenocopies *dpy1* (A) Immunoblot detection of SiBZR1-GFP in two representative *SiBZR1* overexpressing transgenic plants (OX-1 and -2) using an anti-GFP antibody. (**B**) Overexpression of *SiBZR1* resulted in a severe droopy leaf phenotype at the seedling (upper) and adult (lower) stage compared with the WT. Bar = 10 cm.

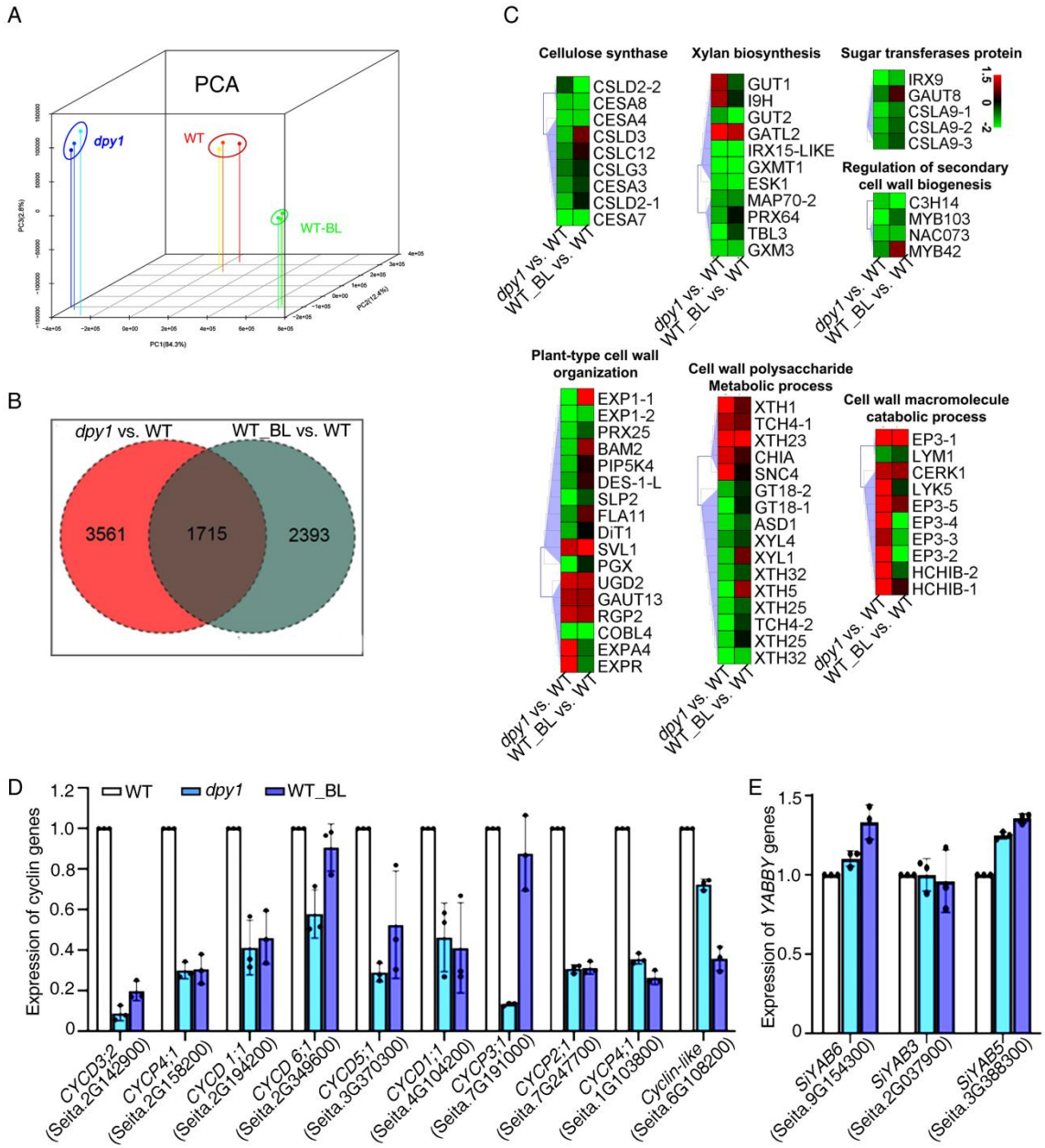

Fig. S11. RNA-seq analysis suggested that *DPY1* functions in the BR pathway and helps regulate cyclin gene expression and cell wall formation. (**A**) Principal component analysis (PCA) of the gene expression data for leaf samples from *dpy1* and WT plants treated with BL or water (mock control). Each group comprises three biological replicates. (**B**) Differentially expressed genes in the leaves of *dpy1* and BL-treated WT plants relative to the expression in mock-treated leaves. A false discovery rate of <0.05 and a fold-change >2.0 were used for the significance cutoff. (**C**) Heat maps visualizing the expression patterns of genes involved in

polysaccharide biosynthesis and wall organization, as well as the cell wall catabolic pathway. (**D** and **E**) Relative transcript abundance of cyclin (D) and *YABBY* (E) family genes in *dpy1* and BL-treated WT plants relative to the WT. The data were pulled from the RNA-seq analysis (n = 3). For each gene, the average CPM (counts per million) value from three biological replicates in WT is set as 1.0.

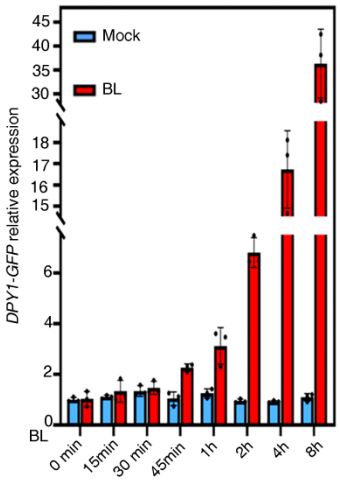

Fig. S12. BL induces *DPY1-GFP* expression. qRT-PCR analysis of *DPY1-GFP* in *DPY1::DPY1-GFP dpy1* transgenic plants treated with 5 μM BL or mock at the indicated time period. The expression level of *DPY1-GFP* in mock-treated plants before treatment was set as 1.0.

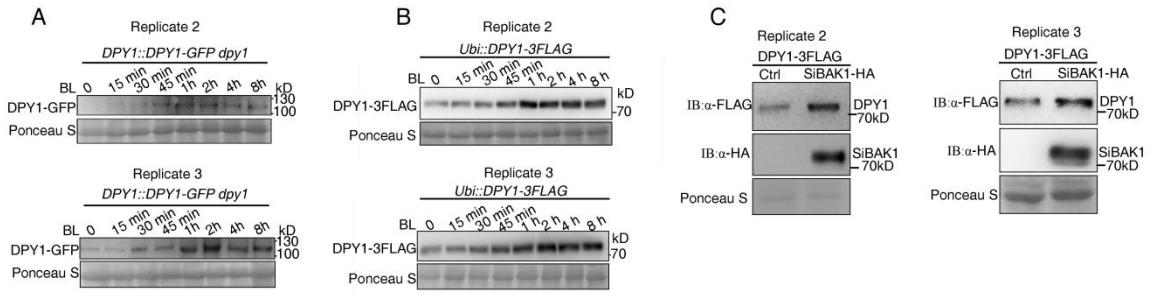

Fig. S13. BL treatment or overexpression of SiBAK1 increases DPY1 accumulation. (**A**) BL-triggered accumulation of DPY1-GFP in *DPY1::DPY1-GFP dpy1* transgenic plants. Ponceau staining served as a loading control. Plants were treated with 5 μM BL at the indicated time period. Biological replicates 2–3 for Fig. 5A. (**B**) BL-triggered accumulation of the DPY1-3FLAG in *Ubi::DPY1-3FLAG* transgenic plants. Ponceau staining served as a loading control. Plants were treated with 5 μM BL at the indicated time period. Biological replicates 2–3 for Fig. 5B. (**C**) SiBAK1 stabilizes DPY1. The *35S::SiBAK1-HA* construct or the empty vector as a control were transiently expressed in *Ubi::DPY1-3FLAG* transgenic protoplasts for 12 h. Protein accumulation was analyzed by immunoblotting with α-HA or α-FLAG antibodies. Biological replicates 2–3 for Fig. 5C.

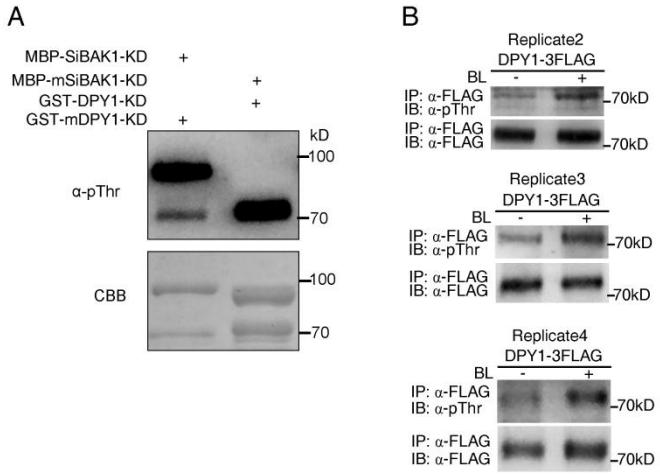

Fig. S14. *In vitro* and *in vivo* examination of DPY1 phosphorylation. (**A**) SiBAK1 phosphorylates DPY1. The MBP-SiBAK1-KD or its kinase-dead version MBP-mSiBAK1-KD protein was incubated with GST-DPY1-KD or GST-mDPY1-KD (kinase-dead version of DPY1) in the presence of ATP. Phosphorylation of GST-mDPY1-KD was detected by immunoblotting with an anti-pThr antibody. (**B**) DPY1 phosphorylation is enhanced by BL. *Ubi::DPY1-3FLAG* transgenic plants treated with or without 10 μM BL was immunoprecipitated (IP) with an α-FLAG antibody and the phosphorylation levels were detected with an anti-pThr antibody (IB). Biological replicates 2–4 for Fig. 5E.

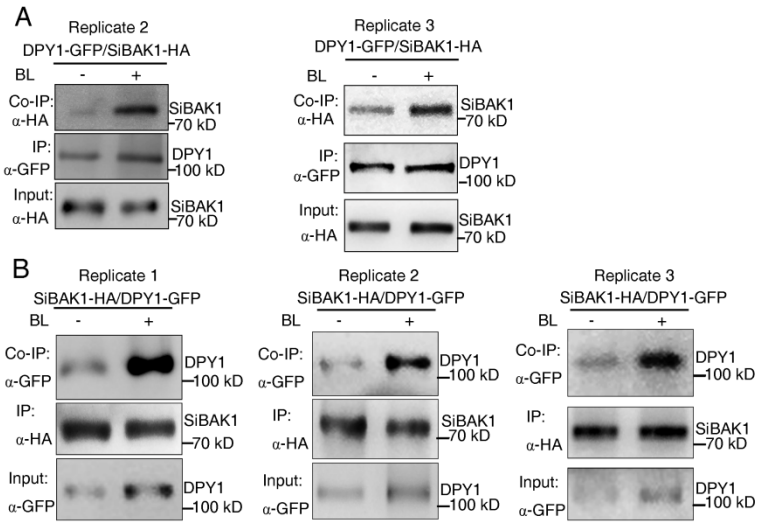

Fig. S15. BL enhances DPY1–SiBAK1 interaction. (**A**) and (**B**) Protoplasts were co-transfected with *35S::DPY1-GFP* and *35S::SiBAK1-HA* for 12 h and incubated with or without 5 μM BL for 2 h. Protein extracts were immunoprecipitated with GFP-Trap beads (IP) and immunoblotted with an α-HA antibody (Co-IP) (A**,** Biological replicates 2–3 for Fig. 5F) or immunoprecipitated with α-HA antibody (IP) and immunoblotted with an α-GFP antibody (Co-IP) (B).

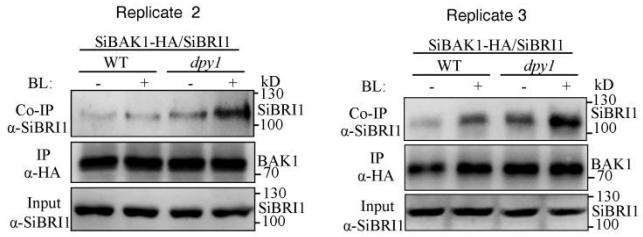

Fig. S16. BL-stimulated SiBRI1–SiBAK1 interaction is enhanced in *dpy1*. Protoplasts from the WT or *dpy1* were transfected with *35S::SiBAK1-HA* for 12 h and incubated with or without 5 μM BL for 2 h. Protein extracts were immunoprecipitated with an α-HA antibody (IP) and immunoblotted with an α-SiBRI1 antibody (Co-IP). Biological replicates 2–3 for Fig. 5G.

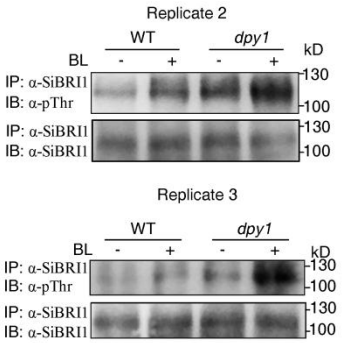

Fig. S17. BL-stimulated SiBRI1 phosphorylation is enhanced in *dpy1*. The *dpy1* and WT plants were treated with or without 5 μM BL. SiBRI1 was immunoprecipitated with an α-SiBRI1 antibody (IP), and its phosphorylation status was determined by immunoblotting with an α-pThr antibody (IB). Biological replicates 2–3 for Fig. 5H.

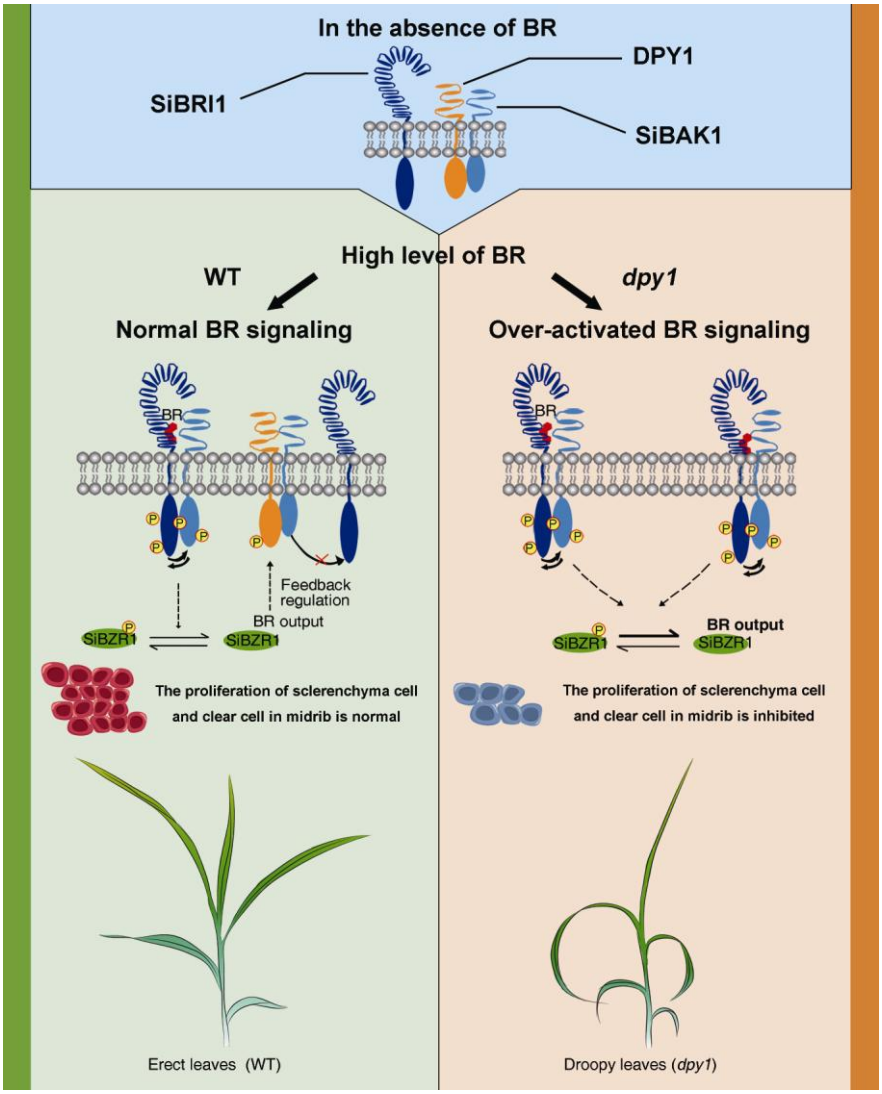

Fig. S18. Proposed model for the DPY1-mediated control of leaf architecture in foxtail millet. In the absence of BRs, DPY1 interacts with SiBAK1 to prevent SiBRI1–SiBAK1 association and downstream signaling initiation. In the presence of BRs, ligand perception induces heterodimerization between SiBRI1 and SiBAK1, forming a stable high-affinity complex, and then they trans-phosphorylate each other to activate SiBRI1. BR signaling transduces from the plasma membrane to downstream components. In a feedback loop, levels of DPY1 and affinity with SiBAK1 increase at the plasma membrane, raising the threshold for SiBRI1–SiBAK1 complex formation, effectively damping BR signaling to ensure normal development of leaf veins for high leaf blade strength. In the absence of DPY1, SiBRI1–SiBAK1 complex formation happens more easily (more co-receptors are available), and thus, generates a stronger BR signaling response, resulting in the malformation of leaf veins, the droopy leaf phenotype, and higher susceptibility to pathogen attack.

Table S1. Compositional analysis of cell walls in wild-type (WT) and *dpy1* leaf blades at the five-leaf stage.

Sample	Rha	Fuc	Ara	Xyl	Man	Gal	Glc	Cellulose	Lignin
WT	5.20	1.72	56.35	179.62	4.03	19.20	37.21	254.43	148.51
	±0.18	±0.05	±1.39	±6.20	±0.12	±0.20	±0.79	±9.52	±6.14
dpy1	4.68	1.65	**45.37**	**159.25**	**3.68**	**14.61**	**31.07**	239.79	**132.74**
	±0.27	±0.04	**±6.67***	**±5.87***	**±0.03****	**±1.15****	**±3.54***	±18.72	**±7.40****

The results indicate the means ± SD. (mg/g alcohol insoluble residues) of three or four (cellulose and lignin) biological replicates. Significant differences were determined using a Student's *t*-test ($^{*}P < 0.05$, $^{**}P < 0.01$) and highlighted with bold values.

Table S2. A list of potential DPY1-interacting proteins identified by IP-MS/MS analysis of the WT and *Ubi::DPY1-3FLAG* over-expressing plants.

Accession number	Intensity WT	Intensity OE	Fold change OE / WT	Description
XP_004968347.1	0	4862400000	-	Immunized bait protein: NSP-INTERACTING KINASE 3 (DPY1)
XP_004956079.1	0	20787000	-	Serine/threonine-protein kinase RAF20 (MAPKKK family)
XP_004963633.1	0	9365800	-	Disease resistance protein RGA2
XP_004965966.1	0	13600000	-	Serine-threonine kinase receptor-associated protein
XP_004968972.1	0	21629000	-	14-3-3-like protein GF14-C
XP_004971044.1	0	12536000	-	AP-4 complex subunit
XP_004952838.2	0	18999000	-	Serine/threonine-protein kinase SAPK6
XP_004979222.1	0	11287000	-	receptor-like kinase TMK4
XP_004964813.1	8321100	33554000	4.03	Mitogen-activated protein kinase 1 (MAPK1)
XP_004957802.1	11765000	46050000	3.91	Protein phosphatase 2C
XP_004978966.1	34154000	86084000	2.52	chitinase 2
XP_004983829.1	155250000	374230000	2.4	Mitogen-activated protein kinase 6 (MAPK6)
XP_012703102.1	3460500	7493400	2.17	Disease resistance protein RGA3
XP_004954168.1	33230000	63301000	1.90	Mitogen-activated protein kinase 5(MAPKK5)
XP_004972726.1	65990000	120270000	1.82	LRR receptor kinase SERK2 (SiBAK1)
XP_004978366.1	97218000	160060000	1.65	Leucine-rich repeat receptor kinase XIAO

Table S3. Content of brassinosteroids (ng / g fresh weight) in leaves 3 and 4 of WT plants at the five-leaf stage

Stage	Content (ng /g FW)				
	BL	CS	6-deo-CS	TY	TE
Five-leaf stage	30.12 ± 2.56	0.72 ± 0.05	1.94 ±0.21	ND	ND

The values indicate the means ± SD from four biological replicates. ND, not detectable; BL, brassinolide; CS, castasterone; 6-deo-CS, 6-deoxocastasterone; TY, typhasterol; and TE, teasterone.

SI References

1. J. L. Bennetzen *et al.*, Reference genome sequence of the model plant Setaria. *Nature biotechnology* **30**, 555–561 (2012).
2. R. Fekih *et al.*, MutMap+: genetic mapping and mutant identification without crossing in rice. *PloS one* **8**, e68529–e68529 (2013).
3. R. C. Edgar, MUSCLE: multiple sequence alignment with high accuracy and high throughput. *Nucleic Acids Res* **32**, 1792–1797 (2004).
4. J. Gui *et al.*, Phosphorylation of LTF1, an MYB Transcription Factor in Populus, Acts as a Sensory Switch Regulating Lignin Biosynthesis in Wood Cells. *Molecular Plant* **12**, 1325–1337 (2019).
5. D. Zhang *et al.*, An Uncanonical CCCH-Tandem Zinc-Finger Protein Represses Secondary Wall Synthesis and Controls Mechanical Strength in Rice. *Molecular Plant* **11**, 163–174 (2018).
6. S. Tang *et al.*, Genotype-specific physiological and transcriptomic responses to drought stress in Setaria italica (an emerging model for Panicoideae grasses). *Scientific Reports* **7**, 10009 (2017).
7. Y. Sun *et al.*, Integration of brassinosteroid signal transduction with the transcription network for plant growth regulation in Arabidopsis. *Developmental cell* **19**, 765–777 (2010).
8. S. Abel, A. Theologis, Transient transformation of Arabidopsis leaf protoplasts: a versatile experimental system to study gene expression. *The Plant Journal* **5**, 421–427 (1994).
9. J. Ji et al., Complementary transcriptome and proteome profiling in cabbage buds of a recessive male sterile mutant provides new insights into male reproductive development. *Journal of Proteomics* **179**, 80–91 (2018).
10. C. M. Carvalho *et al.*, Regulated nuclear trafficking of rpL10A mediated by NIK1 represents a defense strategy of plant cells against virus. *PLoS pathogens* **4**, e1000247–e1000247 (2008).
11. P. Xin, J. Yan, J. Fan, J. Chu, C. Yan, An improved simplified high-sensitivity quantification method for determining brassinosteroids in different tissues of rice and Arabidopsis. *Plant physiology* **162**, 2056–2066 (2013).